URSI GASS 2021, Rome, Italy, 28 August - 4 September 2021

Higher order scattering contributions with surface integral representations for radome analysis

Michael Andersson
Saab Dynamics AB, Sweden

Abstract

This paper presents an analysis technique that has its focus on radome applications, but serves the purpose of being useful for a wider range of scattering problems. The analysis technique is based on classical surface integral representations of the wave fields and the concept of wave propagators, which map the fields from one interface to another. Specifically, higher order scattering contributions are considered by an iterative scheme. The scattered wave fields are found by using reflection and transmission dyadics applicable for general bianisotropic slabs and frequency selective structures (FSS).

1 Introduction

A radome is a cover or structure that encloses an antenna in order to protect the antenna from its physical environment. The presence of the radome enclosing the antenna will introduce distortions of the antenna characteristics in several ways, *e.g.* increased side lobe levels, introduction of boresight error and insertion loss. Many different analysis techniques for the analysis of electrical radome performance exist, ranging from methods with a high degree of approximation towards more accurate techniques, *i.e.* geometrical optics (GO), physical optics (PO) and full wave methods, *e.g.* method of moments (MoM) [1].

Section 2 of this paper reviews and makes use of the classical integral representations in a configuration where the source region is enclosed by a scatterer, *e.g.* a radome-enclosed antenna where higher order scattering contributions are formulated in an iterative scheme. Section 3 presents the numerical verification of the proposed method by comparison with an exact modal series solution.

2 Method

The analysis method is based on classical integral representations of the electromagnetic (EM) fields [2]. The EM fields are assumed to be time-harmonic with $e^{-i\omega t}$ dependence throughout the paper.

2.1 Surface integral representations

As a first step, consider the geometry depicted in Figure 1, *i.e.* a scattering configuration where the source volume V_i is in free space *e.g.* antenna free space configuration.

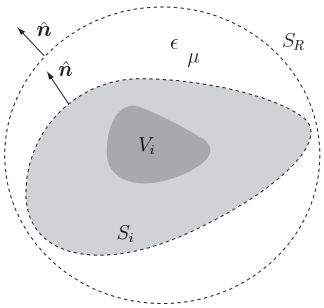

Figure 1. Scattering geometry for source volume V_i in free space.

The free space EM fields $\boldsymbol{E}^i$ and $\boldsymbol{H}^i$ outside any closed bounded smooth surface S_i enclosing the sources are represented by [2, 3]

$$i\frac{\eta_0\eta}{k}\nabla\times\left\{\nabla\times\iint\limits_{S_i}\mathbf{G}(k,|\boldsymbol{r}-\boldsymbol{r}'|)\cdot(\hat{\boldsymbol{n}}(\boldsymbol{r}')\times\boldsymbol{H}^i(\boldsymbol{r}'))dS'\right\}$$
$$+\nabla\times\iint\limits_{S_i}\mathbf{G}(k,|\boldsymbol{r}-\boldsymbol{r}'|)\cdot(\hat{\boldsymbol{n}}(\boldsymbol{r}')\times\boldsymbol{E}^i(\boldsymbol{r}'))dS' \qquad (1)$$
$$=\begin{cases}\boldsymbol{E}^i(\boldsymbol{r}), & \boldsymbol{r}\text{ outside }S_i\\ \boldsymbol{E}^i(\boldsymbol{r})/2, & \boldsymbol{r}\in S_i\\ \boldsymbol{0}, & \boldsymbol{r}\text{ inside }S_i\end{cases}$$

where $k=k_0(\varepsilon\mu)^{1/2}$ is the wave number, $\eta=\sqrt{\mu/\varepsilon}$ is the relative wave impedance, and $k_0=\omega/c_0$ and η_0 are the wave number and wave impedance of vacuum, respectively. The fields $\hat{\boldsymbol{n}}\times\boldsymbol{E}^i$ and $\hat{\boldsymbol{n}}\times\boldsymbol{H}^i$ in the surface integrals are taken as limit values from the isotropic region, *i.e.* from the exterior of S_i. The lower part of the integral representation (1) is usually referred to as the *extinction theorem*. The Green's dyadic $\mathbf{G}$ in an isotropic region is the product of the identity dyadic in three spatial dimensions, $\mathbf{I}_3$, and the Green's function of the scalar Helmholtz equation according to

$$\mathbf{G}(k,r)=\mathbf{I}_3\frac{e^{ikr}}{4\pi r} \qquad (2)$$

This result is the limit as the radius goes to infinity from a contribution of a large sphere with surface denoted S_R, where the fields are assumed to satisfy appropriate radiation conditions [2, 3]. Notice that (1) must be interpreted as a generalized integral due to the singularity of the integrand when $\boldsymbol{r} \in S_i$, see *e.g.* [3].

In a more compact notation (1) is written

$$i\frac{\eta_0\eta}{k}\boldsymbol{K}_{S_i}(\boldsymbol{H}^i)(\boldsymbol{r})+\boldsymbol{L}_{S_i}(\boldsymbol{E}^i)(\boldsymbol{r})=\begin{cases}\boldsymbol{E}^i(\boldsymbol{r}), & \boldsymbol{r}\text{ outside } S_i\\ \boldsymbol{E}^i(\boldsymbol{r})/2, & \boldsymbol{r}\in S_i\\ \boldsymbol{0}, & \boldsymbol{r}\text{ inside } S_i\end{cases} \quad (3)$$

where the integral operators $\boldsymbol{K}$ and $\boldsymbol{L}$ are defined by

$$\begin{aligned}&\boldsymbol{K}_S(\boldsymbol{F})(\boldsymbol{r})\\ &=\nabla\times\{\nabla\times\iint_S \mathbf{G}(k,|\boldsymbol{r}-\boldsymbol{r}'|)\cdot(\hat{\boldsymbol{n}}(\boldsymbol{r}')\times\boldsymbol{F}(\boldsymbol{r}'))dS'\}\end{aligned} \quad (4)$$

and

$$\begin{aligned}&\boldsymbol{L}_S(\boldsymbol{F})(\boldsymbol{r})\\ &=\nabla\times\iint_S \mathbf{G}(k,|\boldsymbol{r}-\boldsymbol{r}'|)\cdot(\hat{\boldsymbol{n}}(\boldsymbol{r}')\times\boldsymbol{F}(\boldsymbol{r}'))dS'\end{aligned} \quad (5)$$

Similarily, the magnetic field can be expressed by [3]

$$-i\frac{1}{k\eta_0\eta}\boldsymbol{K}_{S_i}(\boldsymbol{E}^i)(\boldsymbol{r})+\boldsymbol{L}_{S_i}(\boldsymbol{H}^i)(\boldsymbol{r})=\begin{cases}\boldsymbol{H}^i(\boldsymbol{r}), & \boldsymbol{r}\text{ outside } S_i\\ \boldsymbol{H}^i(\boldsymbol{r})/2, & \boldsymbol{r}\in S_i\\ \boldsymbol{0}, & \boldsymbol{r}\text{ inside } S_i\end{cases} \quad (6)$$

2.2 Scattering contributions

Scattering occurs if there is a region with different material parameters, *i.e.* material parameters that depart from the constant values of ε and μ, [3]. Of interest in this paper is the scattering configuration depicted in Figure 2, where the scatterer, *e.g.* the radome is assumed to be confined to the volume V_s, and the sources within V_i, where V_i does not intersect V_s *i.e.* formally $V_i \cap V_s = \emptyset$.

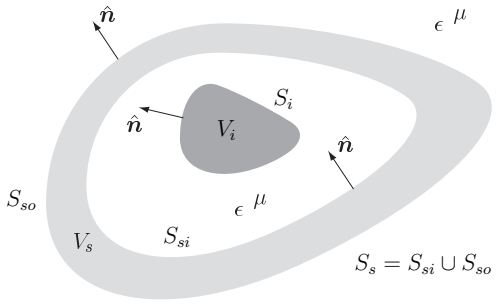

Figure 2. Scattering geometry for scattered EM fields when the source volume V_i is enclosed by the scattering volume V_s.

The space outside the source and scattering regions is assumed to be homogeneous and isotropic with relative permittivity ε and permeability μ, *i.e.* ε and μ are constants. The incident field from the source region, V_i, without the influence of the scatterer is denoted $\boldsymbol{E}^i$ and the presence of the scatterer alters this field by the scattered field $\boldsymbol{E}^s$. Thus, the total field $\boldsymbol{E}$ is

$$\boldsymbol{E}=\boldsymbol{E}^i+\boldsymbol{E}^s \quad (7)$$

A similar notation is used for the magnetic field $\boldsymbol{H}$. Notice that, in general, the presence of the scatterer V_s affects the (real) sources of the incident fields $\boldsymbol{E}^i$ and $\boldsymbol{H}^i$, respectively, *e.g.* if the scatterer is close to V_i [3]. This type of interaction between V_i and V_s is neglected in this paper. Let $\boldsymbol{E}^r$, $\boldsymbol{H}^r$ and $\boldsymbol{E}^t$, $\boldsymbol{H}^t$ denote the reflected and transmitted (scattered) EM fields respectively. The total field $\boldsymbol{E}$ given by (7) is separated into two parts according to

$$\boldsymbol{E}(\boldsymbol{r})=\begin{cases}\boldsymbol{E}^i(\boldsymbol{r})+\boldsymbol{E}^r(\boldsymbol{r}), & \boldsymbol{r}\text{ inside } S_{si}\\ \boldsymbol{E}^t(\boldsymbol{r}), & \boldsymbol{r}\text{ outside } S_{so}\end{cases} \quad (8)$$

and similarly for the total magnetic field $\boldsymbol{H}$. Due to the assumption of no coupling between the sources of V_i and V_s, respectively, we treat the field contributions, *i.e.* the incident (unperturbed), reflected and transmitted EM fields separately. The scattered EM fields for the geometry shown in Figure 2, are found by application of (3)

$$i\frac{\eta_0\eta}{k}\boldsymbol{K}_{S_{so}}(\boldsymbol{H}^t)(\boldsymbol{r})+\boldsymbol{L}_{S_{so}}(\boldsymbol{E}^t)(\boldsymbol{r})=\begin{cases}\boldsymbol{E}^t(\boldsymbol{r}), & \boldsymbol{r}\text{ outside } S_{so}\\ \boldsymbol{E}^t(\boldsymbol{r})/2, & \boldsymbol{r}\in S_{so}\\ \boldsymbol{0}, & \boldsymbol{r}\text{ inside } S_{so}\end{cases} \quad (9)$$

$$i\frac{\eta_0\eta}{k}\boldsymbol{K}_{S_{si}}(\boldsymbol{H}^r)(\boldsymbol{r})+\boldsymbol{L}_{S_{si}}(\boldsymbol{E}^r)(\boldsymbol{r})=\begin{cases}\boldsymbol{E}^r(\boldsymbol{r}), & \boldsymbol{r}\text{ outside } S_{si}\\ \boldsymbol{E}^r(\boldsymbol{r})/2, & \boldsymbol{r}\in S_{si}\\ \boldsymbol{0}, & \boldsymbol{r}\text{ inside } S_{si}\end{cases} \quad (10)$$

and similarily for the magnetic field. The reflected and transmitted EM fields in (9) and (10), respectively, are given in terms of reflection and transmission dyadics $\mathbf{r}_e$, $\mathbf{t}_e$, $\mathbf{r}_h$ and $\mathbf{t}_h$ defined by

$$\begin{cases}\mathbf{r}_e=r_{\parallel\parallel}\hat{\boldsymbol{f}}_\parallel\hat{\boldsymbol{f}}_\parallel+r_{\parallel\perp}\hat{\boldsymbol{f}}_\parallel\hat{\boldsymbol{f}}_\perp+r_{\perp\parallel}\hat{\boldsymbol{f}}_\perp\hat{\boldsymbol{f}}_\parallel+r_{\perp\perp}\hat{\boldsymbol{f}}_\perp\hat{\boldsymbol{f}}_\perp\\ \mathbf{t}_e=t_{\parallel\parallel}\hat{\boldsymbol{f}}_\parallel\hat{\boldsymbol{f}}_\parallel+t_{\parallel\perp}\hat{\boldsymbol{f}}_\parallel\hat{\boldsymbol{f}}_\perp+t_{\perp\parallel}\hat{\boldsymbol{f}}_\perp\hat{\boldsymbol{f}}_\parallel+t_{\perp\perp}\hat{\boldsymbol{f}}_\perp\hat{\boldsymbol{f}}_\perp\\ \mathbf{r}_h=r_{\perp\perp}\hat{\boldsymbol{f}}_\parallel\hat{\boldsymbol{f}}_\parallel+r_{\perp\parallel}\hat{\boldsymbol{f}}_\parallel\hat{\boldsymbol{f}}_\perp+r_{\parallel\perp}\hat{\boldsymbol{f}}_\perp\hat{\boldsymbol{f}}_\parallel+r_{\parallel\parallel}\hat{\boldsymbol{f}}_\perp\hat{\boldsymbol{f}}_\perp\\ \mathbf{t}_h=t_{\perp\perp}\hat{\boldsymbol{f}}_\parallel\hat{\boldsymbol{f}}_\parallel+t_{\perp\parallel}\hat{\boldsymbol{f}}_\parallel\hat{\boldsymbol{f}}_\perp+t_{\parallel\perp}\hat{\boldsymbol{f}}_\perp\hat{\boldsymbol{f}}_\parallel+t_{\parallel\parallel}\hat{\boldsymbol{f}}_\perp\hat{\boldsymbol{f}}_\perp\end{cases} \quad (11)$$

where

$$\begin{cases}\hat{\boldsymbol{f}}_\perp=\hat{\boldsymbol{n}}(\boldsymbol{r}_i)\times\hat{\boldsymbol{k}}^i\\ \hat{\boldsymbol{f}}_\parallel=\hat{\boldsymbol{f}}_\perp\times\hat{\boldsymbol{k}}^i\end{cases}$$

is a set of local basis vectors at each point of observation where $\hat{\boldsymbol{n}}$ and $\hat{\boldsymbol{k}}^i$ denote the normal of S_{si} and power flow direction of the incident EM field at $\boldsymbol{r}_i \in S_{si}$, respectively. The reflection and transmission dyadics (11) map the incident EM fields from one interface to another according to

$$\begin{cases}\boldsymbol{E}^r(\boldsymbol{r}_i)=\mathbf{r}_e\cdot\boldsymbol{E}^i(\boldsymbol{r}_i)\\ \boldsymbol{E}^t(\boldsymbol{r}_o)=\mathbf{t}_e\cdot\boldsymbol{E}^i(\boldsymbol{r}_i)\\ \boldsymbol{H}^r(\boldsymbol{r}_i)=\mathbf{r}_h\cdot\boldsymbol{H}^i(\boldsymbol{r}_i)\\ \boldsymbol{H}^t(\boldsymbol{r}_o)=\mathbf{t}_h\cdot\boldsymbol{H}^i(\boldsymbol{r}_i)\end{cases} \quad (12)$$

where $\boldsymbol{r}_i \in S_{si}$ is corresponding to $\boldsymbol{r}_o \in S_{so}$ by $\hat{\boldsymbol{n}}$. Notice that, the incident EM field on S_{si} of the scatterer is locally considered as a plane wave incident on a planar structure that is stratified in the normal direction $\hat{\boldsymbol{n}}$ at each point of observation $\boldsymbol{r}_i \in S_{si}$. The local plane wave assumption can however be relaxed by using the concept of plane wave spectrum expansion [5, 6].

Slabs that are bianisotropic and either homogeneous, stratified or with continuously varying material parameters as a function of depth can be handled by using relevant wave propagators reported in, *e.g.* [3, 4]. In case of frequency selective structures (FSS), the corresponding reflection and transmission dyadics can be computed by methods reported in, *e.g.* [7, 8, 9].

2.3 Higher order scattering contributions

The fields generated by the sources within V_i are multiple reflected and transmitted by the presence of a scattering volume V_s enclosing the source region V_i illustrated in Figure 2. This section presents an iterative scheme where the integral representations are recursively applied for computation of second and higher order scattering contributions.

By introducing

$$\begin{cases} \boldsymbol{I}^e_S(\boldsymbol{E},\boldsymbol{H})(\boldsymbol{r}) = i\frac{\eta_0\eta}{k}\boldsymbol{K}_S(\boldsymbol{H})(\boldsymbol{r}) + \boldsymbol{L}_S(\boldsymbol{E})(\boldsymbol{r}) \\ \boldsymbol{I}^h_S(\boldsymbol{E},\boldsymbol{H})(\boldsymbol{r}) = -i\frac{1}{k\eta_0\eta}\boldsymbol{K}_S(\boldsymbol{E})(\boldsymbol{r}) + \boldsymbol{L}_S(\boldsymbol{H})(\boldsymbol{r}) \end{cases} \tag{13}$$

we express *e.g.* (3) by

$$\boldsymbol{I}^e_{S_i}(\boldsymbol{E}^i,\boldsymbol{H}^i)(\boldsymbol{r}) = \begin{cases} \boldsymbol{E}^i(\boldsymbol{r}), & \boldsymbol{r} \text{ outside } S_i \\ \boldsymbol{E}^i(\boldsymbol{r})/2, & \boldsymbol{r} \in S_i \\ \boldsymbol{0}, & \boldsymbol{r} \text{ inside } S_i \end{cases} \tag{14}$$

and similarily for the transmitted and reflected EM fields *e.g.* (9) and (10), respectively. Thus, by use of (12) and (14), the first order reflected and transmitted electric fields supported on the inner and outer surfaces S_{si} and S_{so} are written

$$\begin{cases} \boldsymbol{E}^t_1(\boldsymbol{r}_o) = \mathbf{t}_e \cdot \boldsymbol{I}^e_{S_i}(\boldsymbol{E}^i,\boldsymbol{H}^i)(\boldsymbol{r}_i), & \boldsymbol{r}_i \in S_{si}, \quad \boldsymbol{r}_o \in S_{so} \\ \boldsymbol{E}^r_1(\boldsymbol{r}_i) = \mathbf{r}_e \cdot \boldsymbol{I}^e_{S_i}(\boldsymbol{E}^i,\boldsymbol{H}^i)(\boldsymbol{r}_i), & \boldsymbol{r}_i \in S_{si} \end{cases} \tag{15}$$

where S_i is enclosing the source volume V_i depicted in Figure 2. The second order contributions are next found from

$$\begin{cases} \boldsymbol{E}^t_2(\boldsymbol{r}_o)/2 = \mathbf{t}_e \cdot \boldsymbol{I}^e_{S_{si}}(\boldsymbol{E}^r_1,\boldsymbol{H}^r_1)(\boldsymbol{r}_i), & \boldsymbol{r}_i \in S_{si}, \quad \boldsymbol{r}_o \in S_{so} \\ \boldsymbol{E}^r_2(\boldsymbol{r}_i)/2 = \mathbf{r}_e \cdot \boldsymbol{I}^e_{S_{si}}(\boldsymbol{E}^r_1,\boldsymbol{H}^r_1)(\boldsymbol{r}_i), & \boldsymbol{r}_i \in S_{si} \end{cases} \tag{16}$$

Thus, by treating the reflected and transmitted scattering contributions separately in an iterative manner we get for order N

$$\begin{cases} \boldsymbol{E}^t_N(\boldsymbol{r}_o)/2 = \mathbf{t}_e \cdot \boldsymbol{I}^e_{S_{si}}(\boldsymbol{E}^r_{N-1}/2,\boldsymbol{H}^r_{N-1}/2)(\boldsymbol{r}_i), & \boldsymbol{r}_i \in S_{si}, \boldsymbol{r}_o \in S_{so} \\ \boldsymbol{E}^r_N(\boldsymbol{r}_i)/2 = \mathbf{r}_e \cdot \boldsymbol{I}^e_{S_{si}}(\boldsymbol{E}^r_{N-1}/2,\boldsymbol{H}^r_{N-1}/2)(\boldsymbol{r}_i), & \boldsymbol{r}_i \in S_{si} \end{cases} \tag{17}$$

By this procedure the field contributions are accumulated on S_{si} and S_{so} respectively according to

$$\begin{cases} \boldsymbol{E}^t_1(\boldsymbol{r}_o) + \sum_{n=2}^{N} \boldsymbol{E}^t_n(\boldsymbol{r}_o)/2 = \boldsymbol{E}^t(\boldsymbol{r}_o), & \boldsymbol{r}_o \in S_{so} \\ \boldsymbol{E}^r_1(\boldsymbol{r}_o) + \sum_{n=2}^{N} \boldsymbol{E}^r_n(\boldsymbol{r}_i)/2 = \boldsymbol{E}^r(\boldsymbol{r}_i), & \boldsymbol{r}_i \in S_{si} \end{cases} \tag{18}$$

With given scattered near fields on the inner and outer radome surface one readily obtain the corresponding far zone fields, see *e.g.* [3].

3 Numerical results

The SIR[1] method presented in this paper is verified by comparison with an exact modal series solution [10] of a given source configuration in the presence of a spherical radome depicted in Figure 3. The spherical geometry serves as an excellent verification case for various numerical implementations of electromagnetic problems that rely on approximations. This enables an accurate comparison of the approximative method presented in this paper, with the results of this spherical case, which is solved with high accuracy.

The effect of taking into account higher order scattering contributions is seen in Figure 4-6. Figures 4-6 show that higher order scattering contributions are needed in order to accurately model the radiation problem.

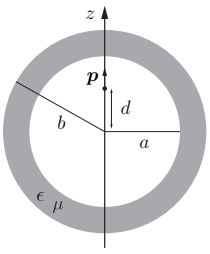

Figure 3. The geometry of the transmission problem of a vertical dipole $\boldsymbol{p}$ inside a spherical shell of inner radius a and outer radius b. The dipole is located at $d\hat{z}$.

4 Conclusions

The presented analysis method combines the classical surface integral representations together with the concept of wave propagators in order to evaluate the distortion of the far field amplitude from a given source enclosed by a scatterer *e.g.* a radome-enclosed antenna. Specifically, an iterative scheme was introduced in order to take into account higher order scattering contributions. Comparison of numerical results with an exact modal series solution to the radiation problem showed that higher order scattering contributions are needed for accurate modelling of the actual source configuration. Furthermore, by use of the concept of wave propagators, the method can handle slabs that in

[1] SIR is an abbreviation for surface integral representation.

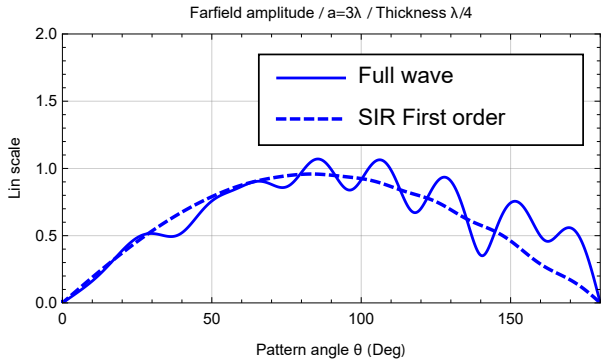

Figure 4. The first order far field amplitude for a vertical dipole at $d = 3\lambda/2$ enclosed by a spherical dielectric shell of radius $a = 3\lambda$ and thickness $\lambda/4$. The dielectric is homogeneous and isotropic with relative permittivity and permeability $\varepsilon/\varepsilon_0 = 3(1+0.01i)$ and $\mu/\mu_0 = 1$, respectively.

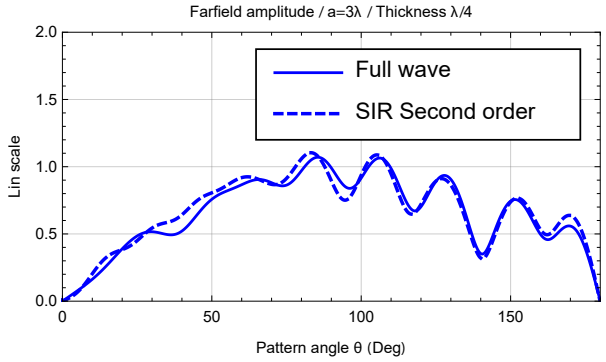

Figure 5. Same as Figure 4, but second order SIR.

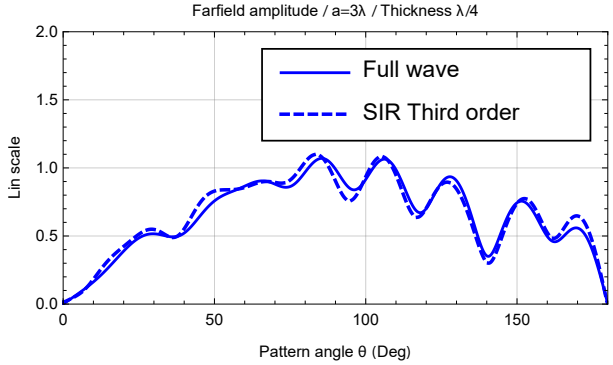

Figure 6. Same as Figure 4, but third order SIR.

general are bianisotropic and either homogeneous, stratified in the direction normal to the surface, *i.e.* laterally homogeneous slabs. The theory is also applicable to frequency selective structures (FSS).

Acknowledgements

The work reported in this paper is supported by grants from the Swedish Defence Materiel Administration (FMV), which are gratefully acknowledged.

References

[1] D. J. Kozakoff, *Analysis of Radome-Enclosed Antennas*, 2nd ed., Artech House, 2010.

[2] S. Ström, Introduction to integral representations and integral equations for time-harmonic acoustic, electromagnetic and elastodynamic wave fields. In V. V. Varadan, A. Lakhtakia, and V. K. Varadan, editors, *Field Representations and Introduction to Scattering*, volume 1 of *Handbook on Acoustic, Electromagnetic and Elastic Wave Scattering*, chapter 2, pages 37-141. Elsevier Science Publishers, Amsterdam, 1991.

[3] G. Kristensson, *Scattering of Electromagnetic Waves by Obstacles*, SciTech Publishing, an imprint of the IET, Edison, NJ, 2016.

[4] S. Rikte, G. Kristensson, and M. Andersson, "Propagation in bianisotropic media – reflection and transmission," *IEE Proc. Microwaves Antennas and Propagat.*, **148**(1), pp. 29–36, 2001.

[5] D. C. F. Wu, and R. C. Rudduck, *Plane wave spectrum – surface integration technique for radome analysis*, IEEE Trans. Antennas Propagat., vol. AP-22, pp. 497–500, May 1974.

[6] M. Andersson, "Plane wave spectrum in radome applications," 2019 International Conference on Electromagnetics in Advanced Applications (ICEAA). IEEE, 2019.

[7] T. K. Wu, *Frequency Selective Surface and Grid Array*, John Wiley & Sons, New York, NY, 1995.

[8] J. C. Vardaxoglou, *Frequency Selective Surfaces (Analysis and Design)*, Research Studies Press, 1997.

[9] B. Munk, *Frequency Selective Surfaces Theory and Design*, John Wiley & Sons, New York, NY, 2000.

[10] G. Kristensson, "Verification of radome problems," Technical Report LUTEDX (TEAT-7262)/1-30/ (2018); Vol. TEAT-7262.